

## Coexistence of in-phase and out-of-phase dynamics in a multimode external-cavity laser diode operating in the low-frequency fluctuations regime

F. Rogister, P. Mégret, O. Deparis, and M. Blondel

*Advanced Research in Optics, Service d'Electromagnétisme et de Télécommunications, Faculté Polytechnique de Mons,  
31 Boulevard Dolez, B-7000 Mons, Belgium*

(Received 27 July 2000; published 15 November 2000)

We study the dynamics of a multimode laser diode with delayed optical feedback operating in the low-frequency fluctuations regime. We show that a multimode extension of the Lang-Kobayashi equations that takes into account spontaneous emission noise predicts two qualitatively different behaviors of the laser on the picosecond time scale. Individual modes of the laser can emit pulses in-phase or oscillate out-of-phase, depending on the operating parameters. The corresponding statistical distributions are in good agreement with two recent experiments.

PACS number(s): 42.65.Sf, 42.60.Mi, 42.55.Px

Subject to external, delayed, optical feedback, laser diodes present a rich variety of dynamical behaviors that can lead to severe degradations of their performances. One of these instabilities is characterized by sudden drop-outs followed by gradual, stepwise recoveries of the optical intensity occurring on a time scale much larger than the period of the relaxation oscillations or the external-cavity round-trip time [1]. For this reason, this regime, which is generally observed when the laser is pumped close to its solitary threshold, is usually referred to as the low-frequency-fluctuations (LFF) regime. External-cavity laser diodes are commonly modeled with the deterministic Lang-Kobayashi equations [2] that assume single-mode operation of the laser and a weak or moderate amount of external optical feedback. Relying on this deterministic model, Sano proposed that the intensity drop-outs are caused by crises between local chaotic attractors and saddle-type antimodes [3]. In his interpretation, the process of the intensity recoveries is associated with a chaotic itinerancy of the system trajectory in phase space among the attractor ruins of external cavity modes, with a drift towards the maximum gain mode close to which collisions with antimodes occur. Further numerical investigations of these equations have anticipated the presence of irregular intensity pulses [4] that have been experimentally confirmed using a streak camera [5]. Moreover, experimental studies have demonstrated the coexistence of the LFF regime with stable emission on a single high-gain external cavity mode in a large range of experimental parameters [6]. The existence of stable external-cavity modes with high gain was previously predicted by an analytical study of the Lang-Kobayashi equations [7]. However, recent experiments [8,9] reveal that, contrary to a major assumption of the Lang-Kobayashi model, multimode operation often occurs within the LFF regime when the laser is not restricted to oscillate in a unique longitudinal mode by a grating or an intracavity etalon. In addition, two recent statistical studies of the laser dynamics on a picosecond time scale have shown that two qualitatively different behaviors may take place within LFF in multimode lasers. In [10], no difference was found between the statistics of single-mode and multimode lasers. By contrast, the statistical distributions experimentally found in [11] suggest fast fluctuations of the total intensity around a nonvanishing av-

erage value, but no pulses. Up to now, both behaviors have not been observed with a unique experimental setup. However, they are predicted by a model based on the Tang, Statz, and deMars equations adapted to laser diodes [12]. In this model, the complex modal fields are coupled to the modal moments of the carrier number that are commonly assumed not to contribute to the laser diode dynamics.

In this Rapid Communication, we investigate numerically the dynamics of a laser diode with optical feedback in the LFF regime by using a multimode extension of the Lang-Kobayashi equations in which the spontaneous-emission noise is taken into account, and the gain is assumed to decrease quadratically from its peak value. Our main purpose is to show that this model predicts two qualitatively different behaviors within the LFF regime, depending on the parameters. Individual modes of the laser may be found to emit pulses in a synchronous way with the consequence that the total intensity exhibits trains of pulses as well. In this case, the calculated probability density distribution of the total intensity is similar to the experimental distributions presented in [10]. However, parameter ranges can also be found within which the longitudinal modes oscillate out-of-phase most of the time. In this case, fast fluctuations of the total intensity around a nonvanishing average value are observed, but no pulses. In agreement with experimental results in [11], the associated probability distribution of the total intensity peaks near its average value and falls off at low and high intensities.

Assuming a parabolic gain profile, the multimode extension of the Lang-Kobayashi equations we use is

$$\frac{dE_m}{dt} = \frac{1}{2}(1 + i\alpha)[G_m(N) - \gamma_m]E_m + \frac{\kappa}{\tau_{Lm}}E_m(t - \tau) \times \exp(-i\omega_m\tau) + F_m(t), \quad (1)$$

$$\frac{dN}{dt} = \frac{J}{e} - \frac{N}{\tau_s} - \sum_m G_m(N)|E_m|^2, \quad (2)$$

where

$$G_m(N) = G_c(N - N_0) \left[ 1 - (m - m_c)^2 \left( \frac{\Delta\omega_L}{\Delta\omega_g} \right)^2 \right].$$

$E_m(t)$  is the slowly varying complex electric field of the  $m$ th mode oscillating at the frequency  $\omega_m$ .  $E_m(t)$  is normalized so that  $I_m(t) = |E_m(t)|^2$  is the photon number in the  $m$ th mode.  $\alpha$  is the linewidth enhancement factor,  $G_m$  and  $\gamma_m$  are the mode-dependent gain coefficient and cavity loss,  $\kappa$  is the feedback level, and  $\tau$  is the round-trip time in the external cavity.  $\omega_m\tau$  is the feedback phase of the  $m$ th mode.  $\tau_{Lm}$  is the round-trip time of the  $m$ th optical mode inside the diode cavity.  $F_m(t)$  is a Langevin noise force that accounts for spontaneous-emission noise.  $N(t)$  is the number of electron-hole pairs inside the active region and  $\tau_s$  is their life time.  $N_0$  is the transparency value of  $N$ .  $J$  is the injection current and  $J_{th}$  the threshold current of the solitary laser.  $e$  is the magnitude of the electron charge.  $G_c$  and  $m_c$  are the gain coefficient and the longitudinal mode number at the gain peak.  $\Delta\omega_L$  and  $\Delta\omega_g$  are the longitudinal mode spacing and the gain width of the laser material, respectively. In our calculations, we assume seven active optical modes and that  $\gamma_m$  and  $\tau_{Lm}$  are mode independent. In this approximation, the mode spacing is given by  $\Delta\omega_L = 2\pi/\tau_{Lm}$ . We use typical values for the laser diode parameters:  $\alpha = 4$ ,  $\gamma_m = 5 \times 10^{11} \text{ s}^{-1}$ ,  $\tau_s = 2 \text{ ns}$ ,  $G_c = 1 \times 10^4 \text{ s}^{-1}$ ,  $m_c = 4$ ,  $N_0 = 1.1 \times 10^8$ , and  $\Delta\omega_g = 2\pi \times 4.7 \text{ THz}$ . The noise level is determined through  $\langle F_m^*(t) F_n(t') \rangle = R_{sp} \delta_{mn} \delta(t - t')$ , where the spontaneous emission rate  $R_{sp} = 1.1 \times 10^{12} \text{ s}^{-1}$ . The feedback phases for the individual modes are given by  $\omega_m\tau = \omega_c\tau + (m - m_c)\Delta\omega_L\tau$ , where  $\omega_c\tau = 0 \text{ mod } 2\pi$  is the feedback phase that corresponds to the central mode. We choose  $\tau_{Lm} = 8.3 \text{ ps}$  so that the feedback phase is different for every mode. The other feedback parameters are  $\kappa = 0.32$  and  $\tau = 3 \text{ ns}$ .

Within the LFF regime, the three longitudinal modes 3, 4, and 5, are dominant, and mode 4, which is located at the maximum of the gain curve, is generally the brightest. By contrast, modes 1 and 7 are depressed most of the time. In agreement with [9,13], the lasing modes are observed to drop simultaneously.

In order to show that two different behaviors on the picosecond time scale can be found, the following will be focused on the dynamics of the total and modal intensities of the laser and their corresponding statistics for two different values of the injection current,  $J = 1.12 \times J_{th}$  and  $J = 1.08 \times J_{th}$ , all the other parameters being kept constant.

Figure 1(a) displays the total intensity for  $J = 1.12 \times J_{th}$ . The time trace has been averaged over 2 ns to model the limited bandwidth of the usual photodetectors used in actual experiments. The average intensity increases steadily with time until it suddenly drops to a minimum value. After the drop-out, the average intensity gradually recovers only to drop again after a random time. On the picosecond time scale, the intensities of the individual longitudinal modes 2 to 6 exhibit fast intensity pulses [Figs. 2(a)–2(c), where only the three brightest modes are shown]. Furthermore, these modes oscillate in phase: they emit pulses with different amplitudes but synchronously. As a consequence, the total in-

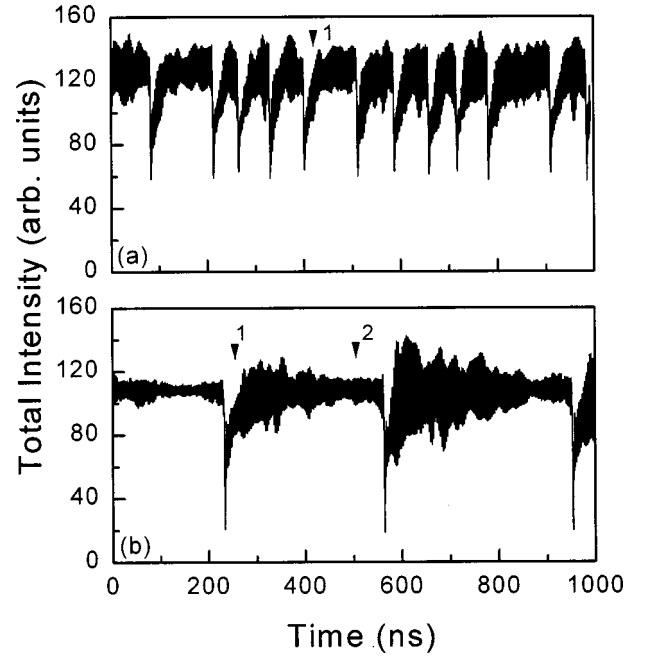


FIG. 1. Time traces of the laser total intensity for two different injection currents: (a)  $J = 1.12 \times J_{th}$ ; (b)  $J = 1.08 \times J_{th}$ . The time traces have been averaged over 2 ns.

tensity exhibits a train of pulses as well [Fig. 2(d)] and shows no qualitative difference with respect to a single-mode laser. The modal synchronization is observed during the entirety of the recovery process, immediately after as well as before a drop-out. In order to compare our numerical results to the experiments, we have calculated the probability den-

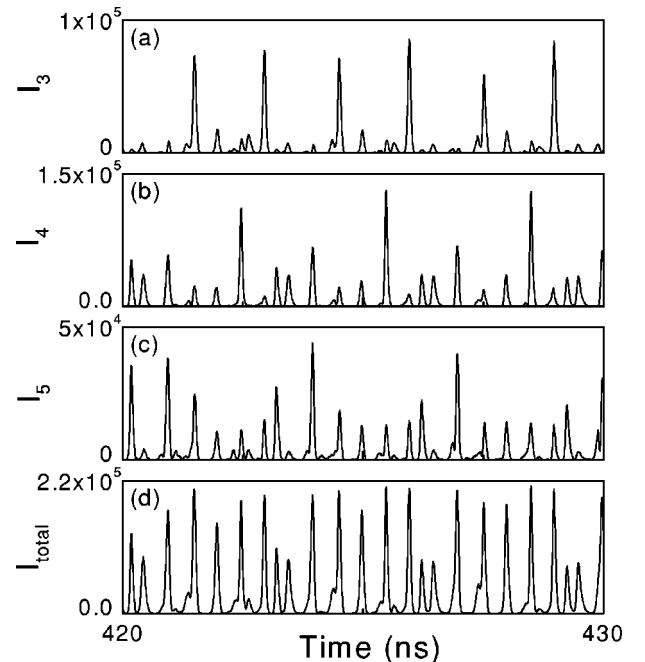


FIG. 2. (a)–(c) Time traces of the unaveraged photon numbers in the three brightest modes; (d) time trace of the total number of photons emitted by the laser. The time segment of the traces corresponds to arrow 1 in Fig. 1(a).  $J = 1.12 \times J_{th}$ .

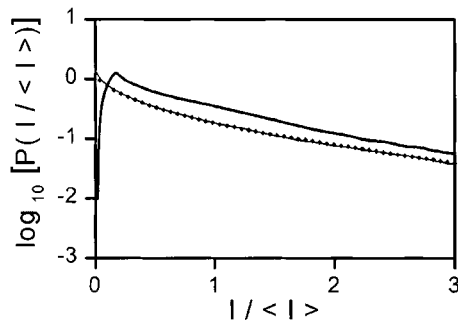


FIG. 3. Probability density distributions of the total laser intensity (thick line), of the center mode (diamonds), and of mode 3 (thin line) intensities. The distributions have been calculated from five time series of 20- $\mu$ s length.  $J = 1.12 \times J_{th}$ .

sity distributions for the total intensity and for the individual longitudinal modes. Figure 3 shows that the distribution corresponding to the total intensity, similarly to the distributions of the individual modes, is maximum at very low intensity and decreases monotonically with increasing intensity. These distributions are characteristic of pulsating behaviors and are in good agreement with the experimental results presented in [10].

For  $J = 1.08 \times J_{th}$ , the mean time interval between two successive drop-outs is considerably longer and the total intensity recoveries are not interrupted by the intensity drop-outs [Fig. 1(b)]. In contrast to the previous case, the average total intensity oscillates around a constant value during long time intervals with respect to the duration of the recovery process. During all the recovery process, the individual modes are pulsing in a synchronous way, similarly to the previous case, and the trains of pulses are also observed in

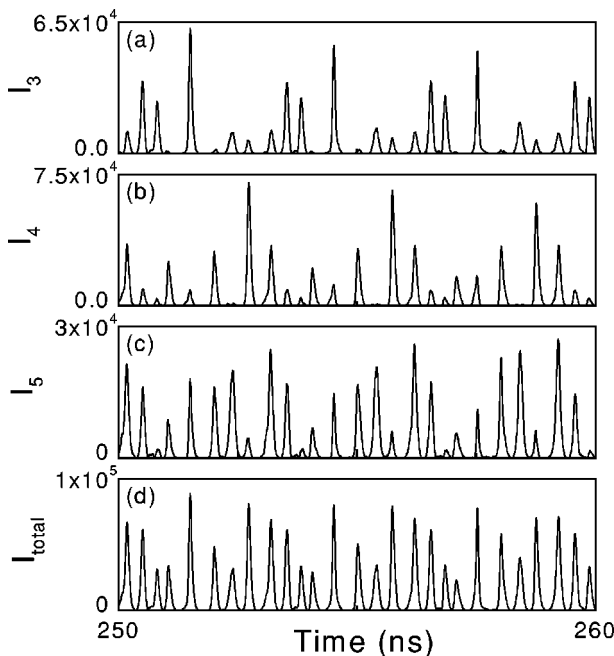


FIG. 4. Same as Fig. 2, but with  $J = 1.08 \times J_{th}$ . The time segment of the traces corresponds to arrow 1 in Fig. 1(b).

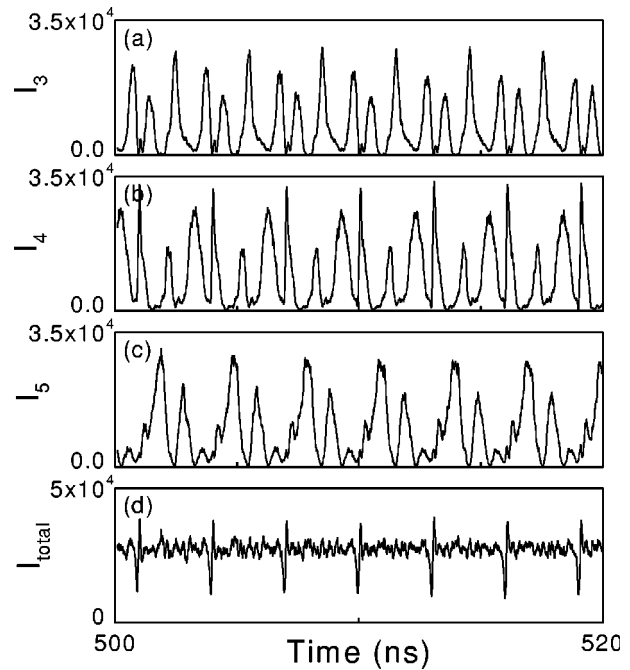


FIG. 5. Same as Fig. 2, but with  $J = 1.08 \times J_{th}$ . The time segment of the traces corresponds to arrow 2 in Fig. 1(b).

the total intensity (Fig. 4). However, as the recovery process ends and the average intensity saturates, the pulses broaden. The modal synchronization is progressively lost and the individual modes are finally observed to oscillate out of phase [Figs. 5(a)–5(c)] with a repetition of an almost similar pattern each round-trip time. An exchange of energy between the individual modes then occurs, leading to a total intensity that is rarely small and exhibits fast fluctuations around a nonzero mean value [Fig. 5(d)], but no more pulses until the next drop-out. Consequently, the probability distribution of the total intensity peaks near its average value and falls off at low and high intensities (Fig. 6). By contrast, the statistical distributions for the individual modes peak at low intensity and exhibit tails showing that pulses with high intensities are observed in each mode while they are not present in the total intensity. These results agree very well with the experimental observations presented in [11].

The two different kinds of behaviors we have pointed out can be found in large ranges of operating parameters, i.e., laser injection current, feedback level, and external cavity

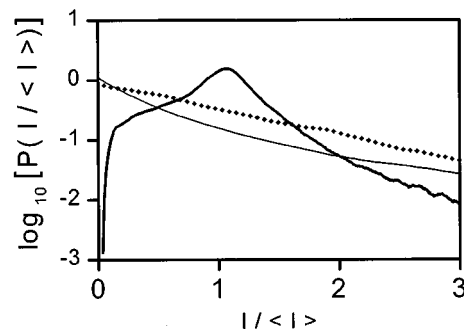


FIG. 6. Same as Fig. 3, but with  $J = 1.08 \times J_{th}$ .

length. By keeping constant the feedback parameters and decreasing continuously the injection current  $J$ , the mean time interval between two consecutive intensity drop-outs increases, in good agreement with experiments involving single and multimode laser diodes [14,15]. The transition between the two behaviors is observed in a small range of the injection current. For the feedback parameters chosen in this study, the transition takes place around  $J=1.10\times J_{\text{th}}$ . Above this value of  $J$ , the first behavior we have depicted, which is a total intensity exhibiting pulses, always occurs. Below this value of  $J$ , the average intensity can recover and reach a constant level around which it oscillates during a long time until the next drop-out. During these long time intervals, the longitudinal modes oscillate out of phase. The fluctuations of the average intensity around a constant level should not be confused with the coexistence of low-frequency fluctuations and stable emission that has been recently reported [6]. Our model allows the observation of stable emission, but in this case the laser operates in a single mode, while the other longitudinal modes are depressed similarly to what has been experimentally reported in [13].

The spontaneous-emission noise plays a crucial role in the multimode dynamics within the LFF regime and the appearance of the out-of-phase dynamics. Indeed, without the noise terms, the laser shares the total intensity among

only the three central modes and does not operate in the surrounding modes. The recovery of the total average intensity is always interrupted by drop-outs before it can reach a plateau and the three remaining modes oscillate always in-phase. On the other hand, the repetition of an almost similar pattern each round-trip suggests that the out-of-phase dynamics is ruled by deterministic mechanisms, although it is initiated by the spontaneous emission noise that is a stochastic process. A possible interpretation of the coexistence of in-phase and out-of-phase dynamics is that the noise allows the system to jump in the phase space between LFF on which the modes oscillate in-phase and a particular attractor that corresponds to the out-of-phase behavior.

In conclusion, we have shown that a multimode extension of the Lang-Kobayashi equations that includes spontaneous emission noise allows one to observe two qualitatively different behaviors of the laser. Depending on the operating parameters, the total intensity exhibits trains of pulses or fluctuates around a nonzero value. The statistical distributions that correspond to both behaviors are in good agreement with recent experiments.

This work was funded by the Inter-University Attraction Pole Program (IAP IV/07) of the Belgian government.

- 
- [1] C. Risch and C. Voumard, *J. Appl. Phys.* **48**, 2083 (1977).
  - [2] R. Lang and K. Kobayashi, *IEEE J. Quantum Electron.* **QE-16**, 347 (1980).
  - [3] T. Sano, *Phys. Rev. A* **50**, 2719 (1994).
  - [4] G. H. M. van Tartwijk, A. M. Levine, and D. Lenstra, *IEEE J. Sel. Top. Quantum Electron.* **1**, 466 (1995).
  - [5] I. Fischer, G. H. M. van Tartwijk, A. M. Levine, W. Elsässer, E. Göbel, and D. Lenstra, *Phys. Rev. Lett.* **76**, 220 (1996).
  - [6] T. Heil, I. Fischer, and W. Elsässer, *Phys. Rev. A* **58**, R2672 (1998).
  - [7] A. M. Levine, G. H. M. van Tartwijk, D. Lenstra, and T. Erneux, *Phys. Rev. A* **52**, R3436 (1995).
  - [8] G. Huyet, S. Balle, M. Giudici, C. Green, G. Giacomelli, and J. Tredicce, *Opt. Commun.* **149**, 341 (1998).
  - [9] G. Vaschenko, M. Giudici, J. J. Rocca, C. S. Menoni, J. Tredicce, and S. Balle, *Phys. Rev. Lett.* **81**, 5536 (1998).
  - [10] D. W. Sukow, T. Heil, I. Fischer, A. Gavrielides, A. Hohl-AbiChedid, and W. Elsässer, *Phys. Rev. A* **60**, 667 (1999).
  - [11] G. Huyet, J. K. White, A. J. Kent, S. P. Hegarty, J. V. Moloney, and J. G. McInerney, *Phys. Rev. A* **60**, 1534 (1999).
  - [12] E. A. Viktorov and P. Mandel, *Phys. Rev. Lett.* **85**, 3157 (2000).
  - [13] I. Wallace, Dejin Yu, R. G. Harrison, and A. Gavrielides, *Quantum Semiclass. Opt.* **2**, 447 (2000).
  - [14] T. Heil, I. Fischer, W. Elsässer, J. Mulet, and C. R. Mirasso, *Opt. Lett.* **24**, 1275 (1999).
  - [15] D. W. Sukow, J. R. Gardner, and D. J. Gauthier, *Phys. Rev. A* **56**, R3370 (1997).